

Heat-Diffusion Central Peak in the Elastic Susceptibility of KSCN

W. Schranz and D. Havlik

Institut für Experimentalphysik der Universität Wien, A-1090 Wien, Austria
(Received 27 April 1994)

We present the first low frequency (0.1–20 Hz) measurements of the complex elastic constant on KSCN single crystals. Our measurements show very slow sample-size dependent elastic relaxations, at temperatures ranging from $T_c - 40$ K up to the order-disorder phase transition temperature T_c . The data can be well explained with the assumption of temperature or equivalent entropy fluctuations. This phenomenon, although intimately related to the thermal-diffusion central peak phenomenon is, to our knowledge, for the first time seen in a macroscopic elastic susceptibility.

PACS numbers: 64.60.Cn, 05.70.Ln, 44.30.+v, 62.20.Dc

Potassium thiocyanate (KSCN) is a model crystal for studying order-disorder phase transitions [1]. A first order phase transition at $T_c = 415$ K leads the crystal from a disordered tetragonal (D_{4h}^{18}) high temperature phase to an ordered antiferrodistortive orthorhombic (D_{2h}^{11}) low temperature phase [2]. Distinct precursor effects preface this phase transition in both phases. From neutron scattering it was found that in the low temperature phase the precursor clusters appear already 40 K below T_c [3]. They consist of small dynamic domains which are in an antiphase relation with the long range ordered matrix of the crystal [3]. The average cluster size $\xi^- \approx 20$ Å depends weakly on temperature and their lifetime $\tau_\eta^- > 10^{-11}$ s. At T_c the long range order parameter η vanishes, but short range order persists up to the melting point, i.e., $T_c + 30$ K [3]. NMR measurements have shown that these short range ordered clusters consist of dynamic orthorhombic microdomains with a lifetime $10^{-5} < \tau_\eta^+ < 10^{-2}$ s [4]. According to diffuse neutron scattering the correlation length $\xi^+ \approx 35$ Å at $T_c + 2$ K and decreases with increasing temperature [3].

To obtain additional insight into the dynamics of the phase transition we performed detailed low frequency ($f = 0.1$ –20 Hz) three-point bending measurements of the complex elastic constant in KSCN. We found a very distinct, probe geometry dependent relaxational process at very low frequencies. For example, for a sample with thickness $h = 0.6$ mm the relaxation time is $\tau_{th} \approx 10^{-1}$ s. By varying the thickness h of the sample the relation $\tau_{th} = (\pi^2 D)^{-1} h^2$ is obtained yielding $D = 2.8 \times 10^{-3}$ cm²s⁻¹. Since this value of D is typical for the thermal diffusivity constants of similar crystals we attribute the observed low frequency dispersion of the elastic susceptibility to a crossover from the isothermal limit ($\omega \tau_{th} \ll 1$) to the adiabatic limit ($\omega \tau_{th} \gg 1$) which occurs because of the effect of temperature (entropy) fluctuations. This effect is closely related to the heat-diffusion “central peak” phenomenon, a subject which was intensively studied in the 1970s by neutron scattering [5] and light scattering [6–9] experiments.

In 1977, Lines and Glass [10] predicted the existence of an ultralow-frequency dispersion due to entropy fluctua-

tions in a macroscopic quantity (dielectric permittivity). Sixteen years later Chaves *et al.* [11] claimed to have observed this phenomenon in the dielectric permittivities of KDP and TGS below their ferroelectric phase transitions. However, they could not verify the q dependence of the relaxation time $\tau_{th}(q) = (Dq^2)^{-1}$, which is characteristic for a heat-diffusion central peak phenomenon.

The KSCN crystals were grown in vessels closed against the open air at 30 °C [12]. They were cut with a diamond saw to obtain rectangular bars with $h = 0.6$ mm (x direction), $t = 2$ mm (y direction), and $l = 7$ mm (z direction). The corresponding lattice constants are $a = 6.691$, $b = 6.676$, and $c = 7.606$ Å at room temperature.

The temperature dependences of the real and imaginary parts of the elastic response to a time dependent stress were measured using a commercial dynamical mechanical analyzer (DMA7, Perkin Elmer) in the frequency range between 0.1 and 20 Hz. With this apparatus one can measure the static and dynamic strain in response to a static or dynamic stress with a resolution of about 3 and 20 nm, respectively. To get a strain amplitude of 1 μm at the rather low force of 100 mN we used the three-point bending mode (Fig. 1). In this mode the bending force results in a stress profile, which in lowest approximation can be written as $\sigma_3(x) \propto \cos(qx)$, where the magnitude of the wave vector q is determined by the size of the sample, i.e., $q = \pi/h$ [13]. The resulting complex elastic constant $C_{33}^{eff}(q, \omega) = C_{33}^{eff}(q, \omega) + iC_{33}^{eff}(q, \omega) = S_{33}^{-1}(q, \omega)$.

Figure 2 shows as an example the temperature dependences of C_{33}^{eff} and C_{33}^{eff} measured at 0.2, 2, and at 10⁷ Hz

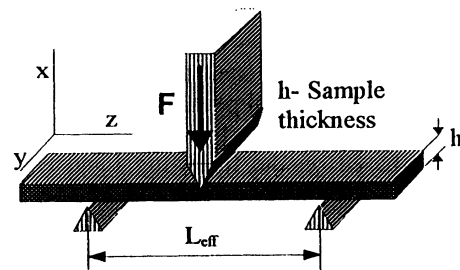


FIG. 1. Three-point bending geometry.

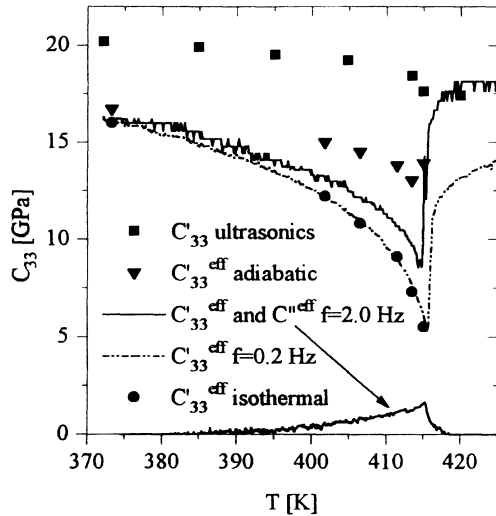


FIG. 2. Measured temperature dependences of the real (C_{33}^{eff}) and the imaginary (C_{33}^{eff}) part of the complex elastic constant for frequencies of 0.2 and 2 Hz. (∇) adiabatic and (\bullet) isothermal elastic constants are obtained from the frequency scans at various temperatures (Fig. 3). The measurements at 10^7 Hz (\blacksquare) were previously performed with ultrasonic technique [14].

(ultrasonic measurement [14]). In addition, the adiabatic and isothermal values extrapolated from frequency scans (Fig. 3) performed at various temperatures are shown. At low frequencies C_{33}^{eff} exhibits a large negative anomaly at T_c . The magnitude of the jump decreases with increasing measurement frequency and is reduced by a factor of about 2 for the adiabatic elastic constant. At ultrasonic frequencies (10^7 Hz) the negative dip vanished completely [14].

Simultaneously with the onset of the dip in C_{33}^{eff} , the imaginary part C_{33}^{eff} of the complex elastic constant increases with increasing temperature, displaying a maximum at T_c . With further heating C_{33}^{eff} falls to zero slightly above T_c . For $h = 0.6$ mm the strongest damping is observed around 1 Hz. To get further information on the dynamics we performed frequency scans for C_{33}^{eff} and C_{33}^{eff} at various temperatures (Fig. 3). The curves are characteristic for a relaxational process with a rather long, slightly temperature dependent relaxation time $\tau_1 \approx 0.1$ s. The connection between the 20 Hz region and the 10 MHz region requires a second relaxational process with $10^{-7} < \tau_2 < 10^{-3}$ s.

In the following we will analyze the data in the frame of a thermal diffusion central peak model [7]. The details of the calculations will be published elsewhere [15]. The theory is based on the following Landau-Ginzburg expansion of the free energy density [1]

$$F = F_0 + \frac{A}{2} (T - T_0)\eta^2 + \frac{B}{4} \eta^4 + \frac{G}{6} \eta^6 + \frac{1}{2} g(\nabla\eta)^2 + \frac{a}{2} \eta^2 \epsilon_3 + \frac{C_{33}^0}{2} \epsilon_3^2 - \sigma_3 \epsilon_3, \quad (1)$$

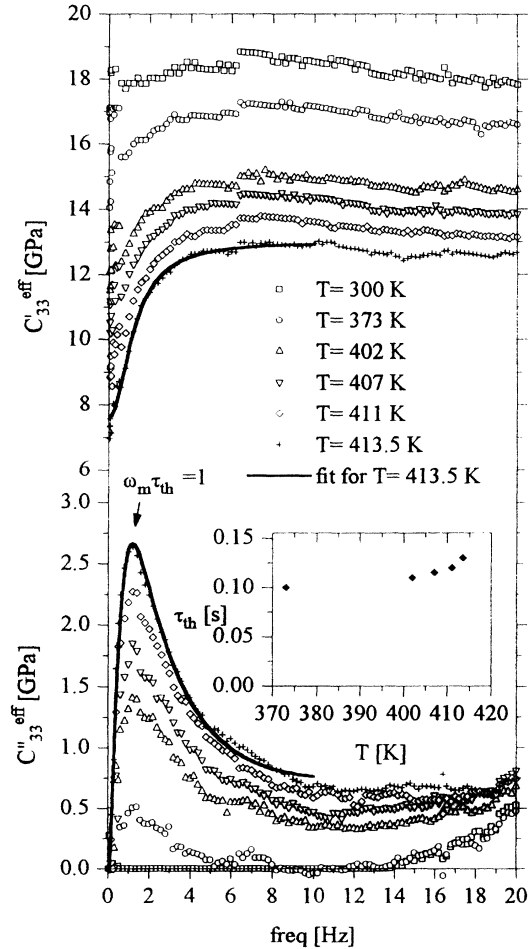


FIG. 3. Measured frequency dependences of C_{33}^{eff} and C_{33}^{eff} at different temperatures below T_c . (—) fit using Eq. (6). Inset: Temperature dependence of τ_{th} .

where η is the primary order parameter describing the orientational ordering of the SCN^- molecules with the critical wave vector $\mathbf{Q}_c = \mathbf{a}^*/2$ [16]. ϵ_3 is the longitudinal strain in Voigt notation and C_{33}^0 is the corresponding bare elastic constant. σ_3 denotes the stress in z direction.

In the presence of $\eta^2 \epsilon$ coupling in (1) the elastic anomaly can be written (neglecting three- and four-point correlations of order parameter fluctuations) as [17]

$$C_{33}(q, \omega) = C_{33}^0 - a^2 \eta_0^2(Q_c) \chi_\eta(q - Q_c, \omega), \quad (2)$$

where $\eta_0^2(Q_c)$ is the equilibrium order parameter. In the presence of a central peak mechanism the order parameter susceptibility χ_η has the following form [7]:

$$\chi_\eta^{-1}(q - Q_c, \omega) = \chi_\eta^{-1LK}(q - Q_c, 0) \times [1 - i\omega\tau_\eta(q - Q_c)] - \frac{\delta^2 i\omega/\gamma}{1 - i\omega/\gamma}. \quad (3)$$

The first part in (3) is the so-called Landau-Khalatnikov term which is obtained from a relaxational

behavior of the order parameter fluctuations, i.e., $\delta\eta(q, t) = \delta\eta(q, 0)e^{-t/\tau_\eta(q)}$. The order parameter relaxation time in (3) is given by

$$\tau_\eta(q - Q_c) = \frac{\tau_\eta(Q_c)}{1 + (q - Q_c)^2 \xi^2}, \quad (4)$$

where ξ is the correlation length of the order parameter fluctuations. The last term in (3) quite generally describes

central peak phenomena of various origins. For a heat-diffusion central peak $1/\gamma$ in (3) is the thermal diffusion time [6,7]

$$\tau_{th}(q) = (Dq^2)^{-1}, \quad (5)$$

where D is the thermal diffusivity constant. $\delta^2 = A^2 \eta_0^2 T / C_\eta$, where C_η is the specific heat at constant η . Inserting (3) into (2) one obtains

$$C_{33}(q, \omega) = C_{33}^0 - \frac{a^2 \eta_0^2(Q_c) \chi_\eta(q - Q_c, 0)}{1 - i\omega \left[\tau_\eta(q - Q_c) + \frac{\delta^2 i\omega \tau_{th}(q) \chi_\eta(q - Q_c, 0)}{1 - i\omega \tau_{th}(q)} \right]}. \quad (6)$$

Equation (6) describes two relaxational processes of a Debye form which are due to fluctuations in the order parameter $\delta\eta(q - Q_c, t) = \delta\eta(q - Q_c, 0)e^{-t/\tau_\eta(q - Q_c)}$ and the temperature $\delta T(q, t) = \delta T(q, 0)e^{-t/\tau_{th}(q)}$. Since in our measurement geometry (Fig. 1) q is determined by the thickness of the sample, i.e., $q = \pi/h \approx 50 \text{ cm}^{-1} \ll Q_c = \pi/a \approx 10^8 \text{ cm}^{-1}$, the order parameter relaxation time τ_η [Eq. (4)] cannot depend on q . In contrast the thermal relaxation time should strongly depend on the size of the sample, i.e., $\tau_{th}(q) = (Dq^2)^{-1} = h^2/D\pi^2$. Frequency scans with probes of various thicknesses (Fig. 4) yield the quadratic dependence of τ_1 on the sample thickness (Fig. 5). In addition the diffusivity constant determined from this fit is in good agreement with the values for thermal diffusivity constants of molecular crystals. This proves, that the low frequency elastic relaxation which we are probing is due to temperature fluctuations along the x direction of our sample, i.e., $\tau_1 = \tau_{th}(q)$. As a consequence the second dispersion observed between the 20 Hz and the 10 MHz region (Fig. 2) is due to the order parameter fluctuations [Eq. (6)], i.e., $\tau_2 = \tau_\eta^-(Q_c) \ll \tau_{th}(q)$. Using Eqs. (3) and (5) one obtains that the thermal diffusion central peak phenomenon leads to a difference between isothermal and adiabatic elastic response. The isothermal limit $\omega\tau_{th} \ll 1$ yields $\chi_T^{-1} = \chi_\eta^{-1LK}(Q_c, 0)$, the inverse

isothermal susceptibility, whereas for $\omega\tau_{th} \gg 1$, $\omega\tau_\eta^- \ll 1$ one obtains the adiabatic limit $\chi_S^{-1} = \chi_\eta^{-1LK}(Q_c, 0) + \delta^2$. Since τ_{th} depends strongly on the q vector sampled by the experimental technique, the crossover from isothermal to adiabatic behavior occurs at different frequencies depending on the experimental method. For a typical light scattering experiment the momentum transfer $q \approx 10^5 \text{ cm}^{-1}$ resulting in $\tau_{th}(q) = 10^{-7} \text{ s}$ for $D = 10^{-3} \text{ cm}^2 \text{ s}^{-1}$ [9]. In our case the extremely small wave vector $q = 50 \text{ cm}^{-1}$ which is given by the thickness h of the sample yields $\tau_{th}(q) = 0.12 \text{ s}$ at $T = 413 \text{ K}$ for $h = 0.06 \text{ cm}$. Thus for $f \ll 1 \text{ Hz}$ the isothermal elastic constant is measured (\bullet in Fig. 2) yielding the full elastic anomaly at T_c [Eq. (6)]. From Fig. 3 it is evident, that the adiabatic elastic constant is measured at frequencies higher than 10 Hz. The large difference between low frequency (20 Hz, \blacktriangledown in Fig. 2) and higher frequency (10 MHz, \blacksquare in Fig. 2) elastic constants is due to a crossover from $\omega\tau_\eta^- \ll 1$ to $\omega\tau_\eta^- \gg 1$ region [Eq. (6)], yielding the order parameter relaxation time $10^{-7} < \tau_\eta^- < 10^{-3} \text{ s}$.

In summary, very slow (1 Hz) elastic relaxations have been found in KSCN below the order-disorder phase transition by low frequency elastic measurements. This

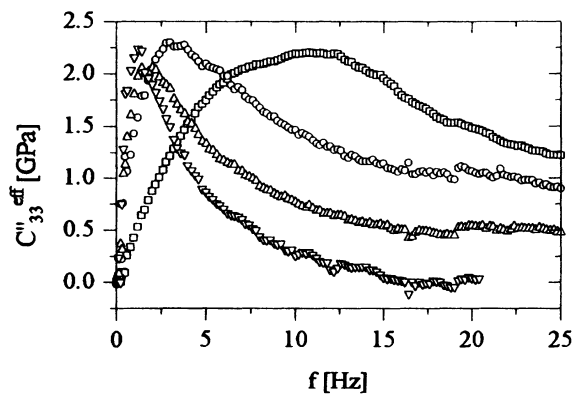


FIG. 4. Frequency dependences of C_{33}^{eff} for various sample thicknesses h measured at $T = 413 \text{ K}$. \square $h = 0.2 \text{ mm}$, \circ $h = 0.38 \text{ mm}$, \triangle $h = 0.5 \text{ mm}$, and ∇ $h = 0.6 \text{ mm}$.

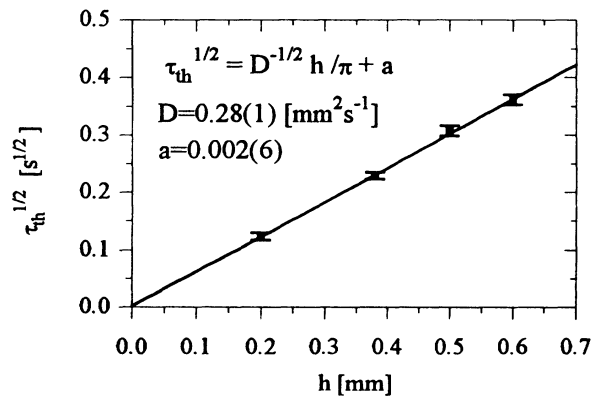


FIG. 5. Thermal diffusion time τ_{th} as a function of the thickness h of the sample, as obtained from the fits of the data of Fig. 4 using Eq. (6). Limits of error are 3σ values.

ultralow frequency dispersion is not caused by order parameter fluctuations. To explain our low frequency (0.1–20 Hz) data another relaxation mechanism is required, which we have shown to originate from entropy fluctuations. The physics of this effect is essentially equal to the thermal-diffusion central peak phenomenon observed, e.g., by light scattering in KDP [9]: Because of the $\eta^2 T$ coupling in the free energy (1) the order parameter fluctuations lead to a term $\eta_0(Q_c)\delta\eta(Q_c - q)\delta T(q)$ creating a spectrum of temperature fluctuations $\delta T(q)$ which propagate with characteristic diffusion times $\tau_{th}(q)$. In a given experiment a particular q component of the temperature fluctuations $\delta T(q)$ is probed. In a scattering experiment $q(\approx 10^5 \text{ cm}^{-1})$ for light scattering is the wave vector transfer to the crystal, whereas in our three-point bending experiment $q(\approx 50 \text{ cm}^{-1})$ is determined by the size h of the sample. This enabled us to verify the sample geometry dependent dispersion $\tau_{th}(q = \pi/h) \propto h^2/D_{th}$, which is characteristic for a heat-diffusion central peak mechanism.

To our knowledge this is the first example for the observation of a thermal diffusion central peak in a macroscopic elastic susceptibility.

We would like to thank A. Fuith for supplying the KSCN crystals. The present work was supported by the Österreichischen Fonds zur Förderung der wissenschaftlichen Forschung under Project No. P8285.

- [1] W. Schranz, *Phase Transitions* **51**, 1 (1994).
- [2] S. Yamamoto *et al.*, *J. Phys. Soc. Jpn.* **56**, 4393 (1987).
- [3] O. Blaschko *et al.*, *Phys. Rev. B* **44**, 9159 (1991); *Ferroelectrics* **124**, 139 (1991).
- [4] R. Blinc *et al.*, *Phys. Rev. B* **43**, 569 (1991).
- [5] T. Riste *et al.*, *Solid State Commun.* **9**, 1455 (1971).
- [6] P. A. Fleury and K. B. Lyons, in *Light Scattering near Phase Transitions*, edited by H. Z. Cummins and A. P. Levanyuk, (North-Holland, Amsterdam, 1983), p. 449.
- [7] E. Courtens and R. Gammon, *Ferroelectrics* **24**, 19 (1980).
- [8] K. B. Lyons and P. A. Fleury, *Phys. Rev. Lett.* **37**, 161 (1976).
- [9] M. D. Mermelstein and H. Z. Cummins, *Phys. Rev. B* **16**, 2177 (1977).
- [10] M. E. Lines and A. M. Glass, in *Principles and Applications of Ferroelectrics and Related Materials*, edited by M. E. Lines and A. M. Glass (Clarendon, Oxford, 1977), p. 130.
- [11] A. S. Chaves *et al.*, *Phys. Rev. B* **47**, 4480 (1993).
- [12] A. Fuith *et al.*, *J. Cryst. Growth* **97**, 469 (1989).
- [13] D. W. Wilson and L. A. Carlson, in *Physical Methods of Chemistry*, edited by B. W. Rossiter and R. C. Baetzold (Wiley, New York, 1991), Vol. VII, p. 178.
- [14] W. Schranz *et al.*, (unpublished).
- [15] D. Havlik and W. Schranz (to be published).
- [16] W. Schranz *et al.*, *J. Phys. Condens. Matter* **1**, 1141 (1989).
- [17] J. O. Fossum, *J. Phys. C* **18**, 5531 (1985).

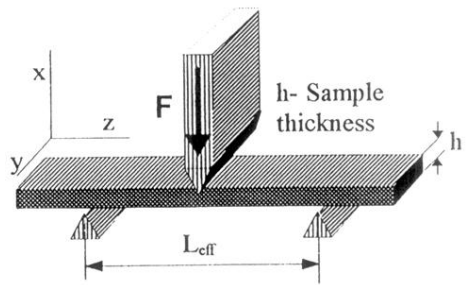


FIG. 1. Three-point bending geometry.